Condensation Reactions between 1,3-Butadiene Radical Cation and Acetylene in the Gas Phase

Guy Bouchoux,*,† Minh Tho Nguyen,‡ and Jean-Yves Salpin†,‡

Laboratoire des Mécanismes Réactionnels, UMR CNRS 7651, Ecole Polytechnique, 91128 Palaiseau Cedex, France, and Department of Chemistry, University of Leuven, Celestijnenlaan 200F, 3001 Leuven, Belgium

Received: March 15, 2000

The present paper reports the first experimental and theoretical results concerning the reaction of [1,3-butadiene]$^{+\bullet}$ radical cation, **1**, with neutral acetylene C_2H_2, **2**. Experiments conducted in the gas phase and under low pressure in an FT-ICR mass spectrometer show that the reaction leads to $C_6H_7^+$ ions. Complete analysis of the experimental data reveals that a mixture of three distinct $C_6H_7^+$ species is produced: it consists of benzenium ions, **a** (≈55%), and the two most stable protonated forms of fulvene (i.e., a-protonated fulvene, **b**, ≈25%, and bicyclo[3,1,0]-hexenyl, **c**, ≈20%). A mechanism, supported by ab initio molecular orbital calculations at the UMP2/6-311+G(d,p)//UMP2/6-31G(d) + ZPE level, is proposed to account for the observations. A Diels−Alder type reaction involving stepwise bond formation is at the origin of ionized 1,4-cyclohexadiene, **5**, the first precursor of the benzenium ion **a**. Starting from **5**, hydrogen-atom migrations and ring-contraction processes generate the precursors of the two other products, **b** and **c**.

Introduction

Pericyclic reactions, and particularly the Diels−Alder reaction, hold an important position among the synthetic methods of organic chemistry. However, it is also well-known that cycloadditions of neutral 1,3-dienes with alcenes or alcynes are efficient reactions only if the frontier molecular orbitals are sufficiently close in energy.[1] This limits the reactant pair to an electron-rich compound and an electron-deficient partner, which present a small HOMO−LUMO energy difference. Means of circumventing this limitation are (i) using a catalyst that reduces the electron density of one reactant or (ii) removing an electron from the system. In the latter case, the more oxidizable reactant is transformed into a radical cation either photochemically, electrochemically, or chemically.[2,3] Moreover, the process may become catalytic if the reaction product is able to regenerate the species responsible for the initial electron transfer ("hole catalysis" concept).[4] The radical-cation-initiated reactions present two major advantages: they allow addition between "non-reactive" neutral reactants, and their reaction rates are several order of magnitude greater than those of the corresponding neutral reactions. For these reasons, radical-cation-initiated pericyclic reactions are considered as promising synthetic tools, and a number of applications have been presented in the literature.[2,3]

Despite this interest, the mechanism of these reactions is poorly documented. A general approach to this question is to study, both experimentally and theoretically, simple prototypical reactions. The most convenient way to obtain experimental information on the intrinsic behavior of the reactants is to examine the reactions occurring in the gas phase, i.e., in the absence of solvent or counterion.[6] It is a major advantage of mass spectrometric techniques to allow the possiblity of monitoring ion−molecule reactions at very low pressure (under single-collision conditions). Moreover, these techniques can provide quantitative kinetic and thermodynamic characteristics of the reaction, together with structural information about the products. Thus, recently, we performed a systematic study of the gas-phase reactions of alkenes and diene radical cations using Fourier transform ion cyclotron resonance (FT-ICR) spectrometry.[7] These reactions result in condensation processes leading eventually to cyclic products. For example, it has been established that the parent gas-phase Diels−Alder reaction involving ionized 1,3-butadiene and ethylene gives ionized cyclopentenyl cation as the major product (Scheme 1).[7c]

The mechanistic aspects of the formation of ionized cyclohexene from ionized 1,3-butadiene and ethylene has recently been investigated theoretically.[5] Further investigations are in progress in order to elucidate the detailed mechanism of the cyclization/dissociation process summarized in Scheme 1.[8]

In this context, it was of interest to examine the homologous Diels−Alder reaction between ionized 1,3-butadiene and neutral acetylene. Surprisingly enough, this simple system has not been studied before. Only the results concerning the metal-mediated reaction of neutral 1,3-butadiene with acetylene in the gas phase has been reported in the literature.[9] Obviously, these experiments concern even-electron organic species and do not involve the radical cations. Here, we report the results of the reaction between [1,3-butadiene]$^{+\bullet}$ and acetylene, with special emphasis on a determination of the structure of the reaction products and a calculation of the reaction energy profile. Experiments were conducted in an FT-ICR mass spectrometer and were complemented by high-level ab initio molecular orbital calculations.

The results of the kinetic experiments, in relation to the relevant thermochemistry, will be discussed first. It will be shown that, apparently, only one reaction leading to $C_6H_7^+$ ions is occurring between [1,3-butadiene]$^{+\bullet}$ and acetylene (reaction I, Scheme 2).

However, a detailed treatment of the experimental data reveals that the $C_6H_7^+$ ions are, in fact, a mixture of the most stable forms of protonated benzene and protonated fulvene. This point

* Author to whom correspondence should be addressed.
† Ecole Polytechnique.
‡ University of Leuven.

10.1021/jp001000o CCC: $19.00
Published on Web 05/31/2000

SCHEME 1

SCHEME 2

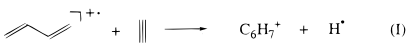

will be presented in the second part. Finally, the thermochemical and mechanistic aspects of the reactions observed are discussed with the help of ab initio molecular orbital calculations conducted at the UMP2/6-311+G(d,p)//UMP2/6-31G(d) + ZPE level for the overall $[C_6H_8]^{+\bullet}$ system and up to the G2(MP2) level for the $[C_6H_7]^+$ product ions.

Experimental Procedure and Computational Details

A. Experiments. Reactions between ionized 1,3-butadiene and acetylene were performed on a Brüker Spectrospin CMS 47X FT-ICR mass spectrometer equipped with an external ion source.[10] [1,3-butadiene]$^{+\bullet}$ ions were produced by electron impact ionization of 1,3-butadiene in the external source (typical conditions were as follows: filament current, 3.5 A; electron energy, 30 eV; and ionization pulse, 10 ms). All ions resulting from electron ionization were transferred to the reaction cell located inside the 4.7 T superconducting magnet. Selection of the ion of interest was accomplished by ejection of all unwanted ions using a combination of broad-band and single-radio-frequency pulses. The isolated reactants were relaxed to thermal energy by introducing argon inside the cell and by imposing a relaxation delay of 4 s after the selection of the reacting ions. Standard experiments were conducted at a constant pressure of acetylene of about 3×10^{-8} mbar, the total pressure in the cell (acetylene plus argon) being 6×10^{-7} mbar. The "gas-phase titration" experiments required a special procedure in which the base B and argon were present inside the cell at a constant pressure. [1,3-butadiene]$^{+\bullet}$ ions formed in the external ion source were selected, relaxed to thermal energy by collision with argon during 2 s, and allowed to react with acetylene introduced in the cell via a pulsed valve. The opening delay of the pulsed valve was optimized so as to obtain a peak pressure of C_2H_2 of 10^{-5} mbar for a few milliseconds. After a pumping delay of 1.25 s, $C_6H_7^+$ product ions were in turn selected, thermalized by collisions with argon during an additional 2 s, and finally allowed to react with the reference base for a variable reaction time.

The bimolecular rate constant was deduced from the slope of a logarithmic plot of the reactant ion abundance vs reaction time. The concentration of the neutral was determined from its pressure, as indicated by an ion gauge located between the ICR cell and the turbomolecular pump. The reading of the ion gauge was calibrated and corrected for its sensitivity with respect to acetylene.[11]

The reactants, 1,3-butadiene and acetylene, were purchased from Messer Griesheim (Düsseldorf, Germany) and Air liquide (Paris, France), respectively, whereas the deuterated compounds (1,1,4,4-butadiene-d_4 and C_2D_2) were purchased from Eurisotop (CEA, Saint-Aubin, France).

B. Calculations. Ab initio molecular orbital calculations were performed using the Gaussian 94 set of programs.[12] The different structures were first optimized at the Hartree−Fock (HF) level with the d-polarized 6-31G(d) basis set. Harmonic frequencies were determined at this level in order to characterize stationary points as minima (equilibrium structures) or saddle points (transition structures); these frequencies were then scaled by a factor 0.9135 in order to estimate the zero-point vibrational energy (ZPE) or by 0.8953 in the RRKM calculations.[13] Improved geometries were subsequently obtained through calculations using correlated wave functions at the second-order Møller−Plesset perturbation theory (MP2) level with the 6-31G(d) basis set. Finally, relative energies were refined by using the 6-311+G(d,p) basis set and MP2 theory. The unrestricted formalism (UHF, UMP2) was employed for open-shell species, with all electrons being considered for the correlations. Throughout this paper, total energies are expressed in hartrees and relative energies in kJ/mol. Unless otherwise noted, the relative energies given hereafter for the $[C_6H_8]^{+\bullet}$ system are those obtained from UMP2/6-311+G(d,p) total energies and corrected with zero-point vibrational energies (ZPE). Finally, to obtain reliable deprotonation energies and heats of formation for the $C_6H_7^+$ ions, we used the G2(MP2) procedure,[14] which have already proved to give calculated deprotonation energies in very good agreement with experimental values.[15]

Results and Discussion

A. Reactions between [1,3-Butadiene]$^{+\cdot}$ and Acetylene. Reactions between the four pairs of reactants, A−D, were examined.

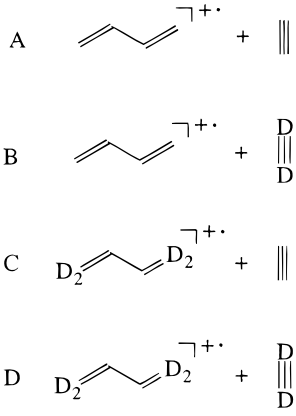

As usual in ion cyclotron resonance mass spectrometry experiments, no signal was detected at the *m*/*z* ratio corresponding to the adduct ions $[C_6H_8]^{+\bullet}$ (or equivalent deuterated species). The low pressure imposed in the ICR cell prevents any efficient collisional deactivation of the intermediate complex, which, in fact, dissociates more readily than it deactivates. Only one type of product ion was identified by the detection of a signal at *m*/*z* 79, corresponding to hydrogen loss from the transient collision complex (reaction I, Scheme 2).

Table 1 summarizes the relative abundances of the $C_6H_xD_{7-x}^+$ ($x = 1-7$) product ions generated from reactants A−D. These relative abundances are independent of the reaction time, which was varied from 0 to 20 s. Reactants B, C, and D lead to two product ions corresponding to the loss of either a hydrogen or a deuterium atom. Reactants B give rise to product ions at *m*/*z* 80 and 81 ($C_6H_6D^+$ and $C_6H_5D_2^+$, respectively), with a ratio of ion abundances of 23%/77%. This ratio matches closely a situation in which one hydrogen is selected from a statistical distribution of six hydrogen and two deuterium atoms (25%/75%). However, the ratios of H or D losses from reactants C and D indicate that the H/D scrambling is not statistical, as these two reactions seem to favor the loss of a H atom with respect to a statistical distribution of the label. No simple model involving specific isotope effects and hydrogen exchanges appears to account for the experimental data. Obviously, this

TABLE 1: Product Ion Abundances and Rate Constant for Reactions between Ionized Butadiene and Acetylene

	relative abundances of product ions (%)[a]									
reactants	$C_6H_7^+$	$C_6H_6D^+$	$C_6H_5D_2^+$	$C_6H_4D_3^+$	$C_6H_3D_4^+$	$C_6H_2D_5^+$	$C_6HD_6^+$	k_{exp}[b]	k_{coll}[b]	RE[c]
$[CH_2CHCHCH_2]^{+\bullet} + C_2H_2$	100							0.73	10.20	0.071
$[CH_2CHCHCH_2]^{+\bullet} + C_2D_2$		23 (25)	77 (75)					0.90	9.95	0.090
$[CD_2CHCHCD_2]^{+\bullet} + C_2H_2$				37 (50)	63 (50)			0.87	10.09	0.086
$[CD_2CHCHCD_2]^{+\bullet} + C_2D_2$						56 (75)	44 (25)	0.98	9.83	0.100

[a] Abundances corresponding to a statistical scrambling of all hydrogen and deuterium atoms prior to dissociation are indicated in parentheses. [b] Rate constants expressed in 10^{-10} cm^3 molecule^{-1} s^{-1}. [c] Reaction efficiency, RE $= k_{exp}/k_{coll}$.

observation suggests a complex reaction pathway connecting ionized 1,3-butadiene plus acetylene to the $C_6H_7^+$ product ions.

Table 1 also includes the experimental rate constants, k_{exp}, for each reaction. An average experimental rate constant of $k_{exp} = 0.87 \pm 0.09$ cm^3 molecule^{-1} s^{-1} can be deduced from the four experiments. The use of a polarizability value of 3.30 Å^3 for acetylene[16] allows for the Langevin collision rate constant,[17] k_{coll}, to be estimated. It appears that the observations correspond to a reaction efficiency RE $= k_{exp}/k_{coll} \approx 9\%$. This value is small compared to that of the iron-mediated cycloaddition process (95%[9]), but it is about four times as large as that observed when ethylene is used in place of acetylene.[7c]

B. Characterization of the $C_6H_7^+$ Product Ions. To describe the reaction observed, a knowledge of the structure of the $C_6H_7^+$ ions is necessary. As will be immediately shown, the usual means of ion structure characterization (collisional experiment, deuterium labeling) failed in the present case. In fact, the formation of a mixture of $C_6H_7^+$ ions is demonstrated by using the kinetic and thermochemical properties of the system considered, as explained in the two last paragraphs of this section.

1. Collisional Activation and Deuterium-Labeling Experiments. To characterize an ion structure by collisional experiments, it is necessary to have in hand the spectra of the various possible isomers. Unfortunately, these are not available for the $C_6H_7^+$ ions: only the collisional activation (CA) spectrum of the benzenium ion has previously been obtained in FT-ICR experiments and reported in the literature.[18] The reason for this lack of information is the absence of a mode of formation of $C_6H_7^+$ ions that has a pure, given structure in the gas phase. The only exception is the benzenium ion, which is thought to be produced by various means, namely, protonation of benzene itself or dissociation of ionized cyclohexadienes of low internal energy.[18,19]

We have compared the CA spectra of the $C_6H_7^+$ ions prepared (i) from reaction I and (ii) from protonation of the benzene molecule by the isopropyl cation. In the latter case, and according to the nearly identical proton affinity values of propene and benzene,[20] the benzenium ions have only a small amount of internal energy, if any, and should not undergo isomerization. We observe that, under identical FT-ICR experimental conditions, similar spectra are obtained from both means of formation of the $C_6H_7^+$ ions. Four peaks are observed at *m*/*z* 77, 51, 39, and 27, in close agreement with the data of Herman et al.[18] However, we note that the intensities of the latter two peaks are highly sensitive to the collision gas presssure (they represent 25% of the total fragment ion current at a pressure of Ar equal to 5×10^{-8} mbar but disappear completely at 5×10^{-7} mbar). Thus, the use of the CA spectra is restricted to only two peaks corresponding to the loss of H_2 from the parent ions and a subsequent loss of C_2H_2. This is certainly not sufficient to assign unambiguously the benzenium structure to the ions produced by reaction I. Moreover, these experiments do not allow the formation of other ion structures to be discarded.

SCHEME 3

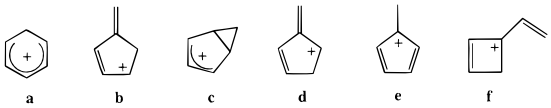

Loss of H_2 also leads to the predominant fragment ion during the metastable[21] and low-energy CA[22] decomposition of $C_6H_xD_{7-x}^+$ ($x = 1-6$) benzenium ions. Moreover, labeling experiments indicate that this fragmentation is preceded by a statistical scrambling of the seven hydrogen atoms. Consequently, we also performed CID experiments for the six $C_6H_xD_{7-x}^+$ ($x = 1-6$) ions formed during the reactions B, C, or D. The spectra recorded indeed reveal a statistical mixing of the seven hydrogens and deuteriums prior to dissociation. Our results are very close to those deduced from low-energy CA experiments carried out with flow-tube or triple-quadrupole instruments,[22] thus suggesting the possible primary formation of benzenium ions during the reaction between 1,3-butadiene radical cation and acetylene. Again, however, we cannot exclude the parallel formation of other isomeric ions.

2. Heats of Formation. More conclusive information about the structure of the $C_6H_7^+$ ions can be obtained by considering their thermochemistry. First, it must be recalled that, in our FT-ICR experimental conditions, the reactive species are thermalized by collision with the molecules of a bath gas introduced inside the cell at a pressure 20 times greater than that of the reactants. Consequently, the reactions observed during FT-ICR experiments are, in principle, exothermic. This means that, by combining $\Delta_f H°_{298}$(**1**)= 985 kJ/mol,[23] $\Delta_f H°_{298}$(**2**)= 228 kJ/mol,[23] and $\Delta_f H°_{298}(H^\bullet)$= 218 kJ/mol,[23] the 298 K heat of formation of the $C_6H_7^+$ product ions should be less than (or equal to) 995 kJ/mol. According to this requirement, acyclic structures such as $[CHCCH_2CH_2CCH_2]^+$ or $[CH_3CHCCCCH_3]^+$ can be excluded because their heats of formation are greater than 1090 kJ/mol.[19,23] The heat of formation of benzenium ion **a** (the most stable protonated form of benzene, Scheme 2) is known experimentally. Its value, 862 kJ/mol (from the proton affinity of benzene, 751 kJ/mol,[20,24] by using $\Delta_f H°_{298}(H^+)$= 1530 kJ/mol[23] and $\Delta_f H°_{298}$(benzene)= 83 kJ/mol[23]) is clearly below the limiting value of 995 kJ/mol. It has recently been shown[25] that the various protonated forms of fulvene possess heat of formation values in a 120 kJ/mol energy range above that of **a**. Thus, structures **b**−**e** (Scheme 3) are likely to be generated by reaction between ionized 1,3-butadiene and acetylene. It was also of interest to consider the four-membered ring structure, **f**, a protonated form of vinylcyclobutadiene, formally produced by a [1 + 2] cycloaddition process followed by the loss of a hydrogen atom.

The total energies at 298 K of all of the isomers **a**−**f** were calculated by ab initio molecular orbital calculations at the G2(MP2) level. These data were used to estimate the $\Delta_f H°_{298}$ values for species **b**−**f** by adding the calculated 298 K relative energies, ΔE_{298}, to the experimental value $\Delta_f H°_{298}$(**a**) = 862 kJ/mol. This

TABLE 2: Calculated G2(MP2) Thermochemical Data of the $C_6H_6/C_6H_7^+$ System[a]

structure	$E(G2MP2)_{298}$	ΔE_{298}	$\Delta_f H°_{298}$[b]	$PA(C_6H_6)$[c]	$S°_{298}$[g]	$GB(C_6H_6)$[h]
			$C_6H_7^+$			
a	−232.053866	0	[862]	751[d]	290	725[d]
b	−232.041188	+33	895	848[e]	299	819[e]
c	−232.022989	+81	943	800[e]	284	766[e]
d	−232.016788	+98	960	783[e]	301	754[e]
e	−232.006710	+124	986	757[e]	318	734[e]
f	−231.994180	+133	995	1014[f]	318	983[f]
			C_6H_6			
benzene	−231.771741	0	[83]		269	
fulvene	−231.722296	+130	213		288	
vinylcyclobutadiene	−231.620851	+396	479		314	

[a] Total energies are given in hartrees (1 hartree = 2625.50 kJ/mol); relative energies, heats of formation, proton affinities, and gas-phase basicities are given in kJ/mol. [b] $\Delta_f H°_{298}$ values are anchored to the experimental values indicated in brackets. [c] $PA(C_6H_6) = \Delta_f H°_{298}(C_6H_6) + \Delta_f H°_{298}(H^+) - \Delta_f H°_{298}(C_6H_7^+)$. [d] C_6H_6 = benzene. [e] C_6H_6 = fulvene. [f] C_6H_6 = vinylcyclobutadiene. [g] Deduced from vibrational frequencies calculated at the UHF/6-31G* level. [h] $GB(C_6H_6) = PA(C_6H_6) - 298[S°_{298}(H^+) + S°_{298}(C_6H_6) - S°_{298}(C_6H_7^+)]$, with $S°_{298}(H^+) = 108.7$ J mol^{-1} K^{-1}.

procedure leads to the data quoted in Table 2. The results show that all of the $C_6H_7^+$ isomers considered possess a heat of formation lower than 995 kJ/mol. Consequently, none of the structures **a**−**f** can be excluded as the products of reaction I solely on the basis of their heat of formation value.

In a further attempt to identify the actual $C_6H_7^+$ ions structure-(s), we performed proton-tranfer experiments, which allow a gas-phase titration of a mixture of protonated isomers.[19,26]

3. Gas-Phase Ion Titration Experiments. The kinetics of the proton-transfer reaction II

$$AH^+ + B \rightarrow A + BH^+ \qquad \text{(II)}$$

can be used for a quantitative analysis of a mixture of A_iH^+ isomeric structures. If a_{0i} denotes the initial concentration of isomer A_iH^+ and k_i' denotes the pseudo-first-order rate constant for the deprotonation of isomer A_iH^+ by the base B, the total abundance of AH^+ ions at a reaction time t is given by eq III.

$$AH^+(t) = \sum a_{0i} \exp(-k_i' t) \qquad \text{(III)}$$

Roughly, if one considers that the proton transfer is observed only for exoergic processes, reaction II is expected to occur only when the gas-phase basicity GB(B) is greater than the basicity of the less basic isomer A_i. In such circumstances, the time evolution of the A_iH^+ signal is given by eq III, and therefore, a single- or polymodal exponential decay is observed. Conducting these experiments with a series of reference bases B allows for a "gas-phase titration"[26] of the ion mixture and an estimation of the GB of the conjugated bases A_i. In fact, the kinetic curves can be directly examined by a biexponential curve-fitting procedure to separate the AH^+ ion population into two sets of isomeric ions corresponding to conjugated bases A_i that are less and more basic than B. Concerning the $GB(A_i)$ determination, a more careful analysis of the plot of AH^+ vs reaction time is needed, as explained below.

The pseudo-first-order rate constant appearing in eq III is equal to $k_i' = k_{bi}[B]$, where k_{bi} is the bimolecular rate constant of the deprotonation of isomer A_iH^+ by the base B. The concentration [B] can be calculated from the measured static pressure of the base B in the FT-ICR cell. On the other hand, for a proton-transfer reaction such as II, it has been established[27] that, to a good approximation, the bimolecular rate constant obeys a law of the type

$$k_{bi} = k_{coll}/[1 + \exp(\Delta G_i° + \Delta G_a°)/RT] \qquad \text{(IV)}$$

where k_{coll} is the collision rate constant, $\Delta G_i°$ is the free energy change for the deprotonation of isomer A_iH^+ by the base B, and $\Delta G_a°$ is a corrective term close to RT. Fortunately, the parameter possessing the largest effect on k_i', and consequently on $AH^+(t)$, is the free energy change $\Delta G_i°$, i.e., the difference in gas-phase basicities $GB(A_i) - GB(B)$. Consequently, it is possible to determine each $GB(A_i)$ by modeling the time evolution of the AH^+ ion abundance using both relationships III and IV.[28]

TABLE 3: Proportion of Unreactive $C_6H_7^+$ Species Observed during the Reaction $C_6H_7^+ + B \rightarrow C_6H_6 + BH^+$, with Different Bases B

reference base B	GB(B)[a] (kJ/mol)	unreactive population (%)[b]
1,1,1-trifluoroacetone	692.0	100
propene	722.7	41
methanol	724.5	56
methyl cyanide	748.0	51
methyl formate	751.5	42
ethyl formate	768.4	18
isopropyl cyanide	772.8	22
methyl acetate	790.7	25
ethyl acetate	804.7	21
diethyl ketone	807.0	20
cyclohexanone	811.2	14
diisopropyl ketone	820.5	2
penta-2,4-dione	836.8	4
mesityloxid	846.9	3

[a] From ref 20. [b] See text for details.

This general procedure was used for the analysis of the mixture of $C_6H_7^+$ ions formed by the reaction between ionized 1,3-butadiene and acetylene, as shown in eq V.

$$C_6H_7^+ + B \rightarrow C_6H_6 + BH^+ \qquad \text{(V)}$$

Results from gas-phase titration experiments are summarized in Table 3 and illustrated in Figure 1. No deprotonation of the $C_6H_7^+$ ions occurs with 1,1,1-trifluoroacetone. With propene, a slow deprotonation is observed, with the intensity of the $C_6H_7^+$ ions decreasing steadily to finally stabilize at about 40% at long reaction times. With methanol, a similar result is obtained, but in this case, the deprotonation process is fast. The same trend is found with methyl cyanide. With methyl formate, a double-exponential decay is observed, indicating that a second population of ions is beginning to transfer a proton to the neutral base. With ethyl formate, a different asymptotic behavior is observed at long reaction times. The unreactive population of $C_6H_7^+$ ions falls to a value of 18% at the end of the reaction. This change shows that, in the presence of ethyl formate, two distinct populations of $C_6H_7^+$ ions react by proton transfer. From ethyl

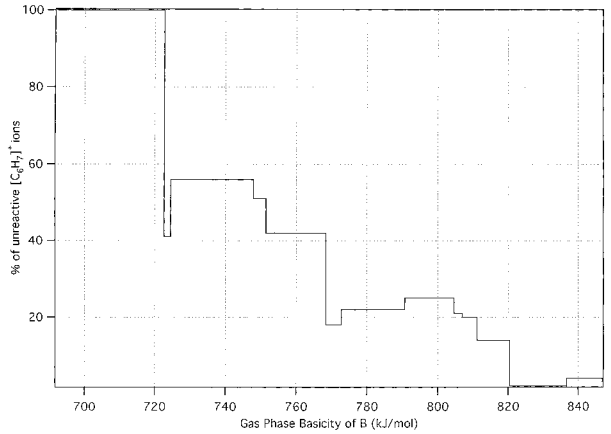

Figure 1. Abundance of unreactive $C_6H_7^+$ ions as a function of the basicity of B, during the proton-transfer reaction $C_6H_7^+ + B \rightarrow C_6H_6 + BH^+$.

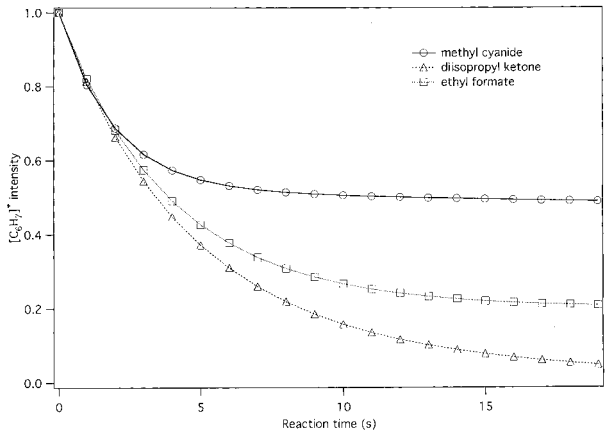

Figure 2. Plot of $C_6H_7^+$ ion abundance versus reaction time for the proton-transfer reaction $C_6H_7^+ + B \rightarrow C_6H_6 + BH^+$ (B = methyl cyanide, diisopropyl ketone, and ethyl formate).

formate to diethyl ketone, the percentage of unreactive ions always lies in the vicinity of 20%. With cyclohexanone, a bimodal behavior is observed. After a few seconds, the two first reactive species are completely deprotonated. At longer reaction times, the abundance of $C_6H_7^+$ ions continues to decrease slowly, thus indicating that a third population starts to react by proton transfer. Finally, a negligible population of unreactive $C_6H_7^+$ ions (2%) is deduced from the kinetics of reactions involving more basic species, such as diisopropyl ketone, penta-2,4-dione, and mesityloxid, for which a fast deprotonation is observed. Three examples of the curve describing $C_6H_7^+$ ion abundance vs reaction time are presented in Figure 2. The asymptotic behavior revealing the different unreactive populations is clearly apparent in these curves. A general view of the abundance of the unreactive $C_6H_7^+$ ions population as a function of the gas-phase basicity of B is presented in Figure 1. It clearly shows the formation of three different sets of $C_6H_7^+$ ions via reaction I.

The detailed treatment of the data using eqs III and IV and the GB(B) values reported in Table 3 confirms that three different $C_6H_7^+$ ions structures are generated by the reaction between $[1,3\text{-butadiene}]^{+\bullet}$ and acetylene. The first population comprises 55 ± 5% of the $C_6H_7^+$ ions and corresponds to $GB(C_6H_6) = 720 \pm 2$ kJ/mol. The second isomer represents 25 ± 5% of the $C_6H_7^+$ ions, and its conjugated base possesses a $GB(C_6H_6)$ value of 766 ± 3 kJ/mol. The third component (20 ± 5%) corresponds to a C_6H_6 species with $GB(C_6H_6) = 820 \pm 2$ kJ/mol. The three sets of $C_6H_7^+$ ions can now be identified

SCHEME 4

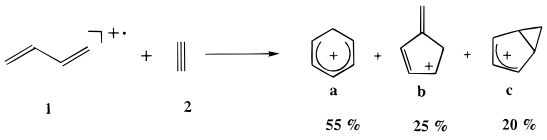

from a comparison of the experimental $GB(C_6H_6)$ values and the expectations based on molecular orbital calculations.

The theoretical $GB(C_6H_6)$ values associated with the various deprotonation processes involving ions **a**−**f** are presented in Table 2. Gas-phase basicity values were calculated using $GB(C_6H_6) = PA(C_6H_6) - 298[S°_{298}(H^+) + S°_{298}(C_6H_6) - S°_{298}(C_6H_7^+)]$, with $S°_{298}(H^+) = 108.7$ J mol^{-1} K^{-1} and $PA(C_6H_6) = \Delta_f H°_{298}(C_6H_6) + \Delta_f H°_{298}(H^+) - \Delta_f H°_{298}(C_6H_7^+)$. The heat of formation values are those listed in Table 2 and obtained by the procedure outlined above. It must be emphasized that the G2(MP2) calculations presented in Table 2 are in very good agreement with experiment. For example, the calculated proton affinity of benzene (751 kJ/mol in Table 2) is in excellent agreement with the most recent experimental value determined by Szulejko and McMahon (751.5 kJ/mol).[24]

As indicated in Table 2, the six species **a**−**f** have distinct free energies of deprotonation, $GB(C_6H_6)$. Therefore, their structural assignment is straightforward. The major population having a $GB(C_6H_6)$ value of 720 kJ/mol should correspond to benzenium ion **a**. The remaining minor population is actually a mixture of both structures **b** (25%) and **c** (20%). Finally, this work also suggests that the $C_6H_7^+$ ions of high energy, namely **d**−**f**, are not generated to a significant extent during reaction I. A summary of the analysis of the experimental results is presented in Scheme 4.

C. Mechanism of Formation of Ions a, b, and c. The last part of this study is devoted to a description of the reaction steps occurring from the reactants, $[1,3\text{-butadiene}]^{+\bullet}$ plus acetylene, to the three products ions **a**, **b**, and **c**. The possible reaction pathways were established by the ab initio methods discussed in Experimental Procedure and Computational Details; a full mechanistic scheme is given in Scheme 5. Selected UMP2/6-31G(d) optimized geometries of the reactants, reaction intermediates, transition structures, and products are presented in Figure 3; the associated bond lengths (b_x) are listed in Table 4. UMP2/6-311+G(d,p)//UMP2/6-31G(d) total and relative energies are quoted in Table 5, together with the $\langle S^2 \rangle$ expectation values, characteristic of the spin contamination in the UHF wave functions. The calculated enthalpies of reaction for each individual step were used to construct the reaction energy profile shown in Figure 4.

As already observed in comparable ion−molecule systems, such as $[1,3\text{-butadiene}]^{+\bullet}$ plus ethylene,[5] $[\text{ethylene}]^{+\bullet}$ plus ethylene,[6f] or $[\text{ethylene}]^{+\bullet}$ plus acetylene,[6g] the two reactants readily collapse to form a stable complex without an energy barrier. During this first step, the approach of $[1,3\text{-butadiene}]^{+\bullet}$ and acetylene gives rise to the ion−neutral complex **3**, which, in turn, may isomerize to **4**. During the latter process, the long-range attractive forces are replaced by a covalent bond, and thus, a critical energy barrier analoguous to that observed in the case of the addition of a carbon-centered radical to an alkene[29] is calculated. The distonic intermediate **4** may further undergo a cyclization to generate the 1,4-cyclohexadiene molecular ion, **5**. These three initial steps formally correspond to an unconcerted [3 + 2] Diels−Alder cycloaddition reaction. The cyclization process is associated with transition structure **TS 4/5**, lying slightly below the enthalpy level of the reactants (−5 kJ/

SCHEME 5

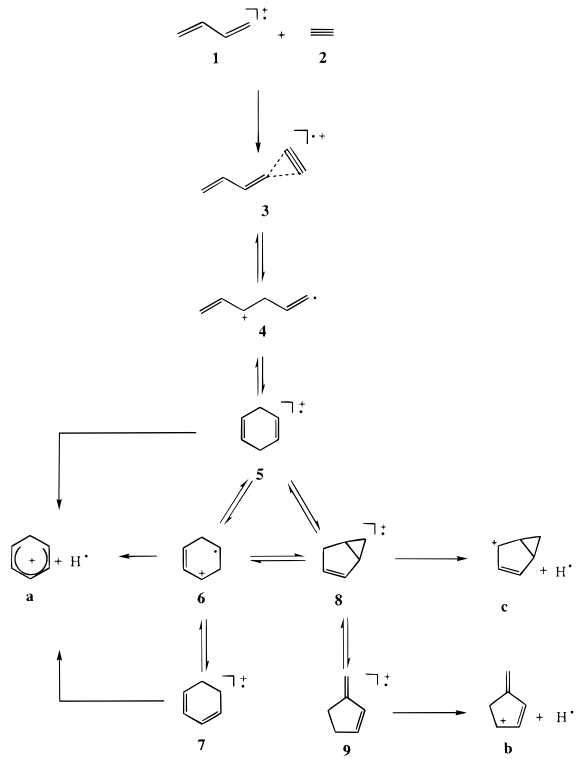

mol) and very close to that of the isomerization **3** → **4**. By no means were we able to locate a transition structure corresponding to a concerted pathway connecting [1,3-butadiene]$^{+\bullet}$ plus acetylene to the 1,4-cyclohexadiene molecular ion, **5**. This observation is in keeping with the recent conclusion that cycloaddition reactions between [1,3-butadiene]$^{+\bullet}$ and ethylene (leading to [cyclohexene]$^{+\bullet}$, [vinylcyclobutane]$^{+\bullet}$, or [methylcyclopentene]$^{+\bullet}$) are stepwise.[5]

Ionized 1,4-cyclohexadiene, **5**, may isomerize by two successive 1,2-H shifts to [1,3-cyclohexadiene]$^{+\bullet}$, **7**, via the distonic species **6**. These three cyclic structures may lead, by hydrogen loss, to the benzenium structure, **a**. However, it is clear from Table 5 and Figure 4 that the loss of a hydrogen from ionized 1,4-cyclohexadiene, **5**, is the most favorable process. The corresponding transition structure, **TS 5/a**, is lower in energy than its possible competitors **TS 6/a** and **TS 7/a** by 62 and 20 kJ/mol, respectively. Ab initio calculations also indicate that the distonic ion **6** should preferentially undergo a ring contraction, leading to the bicyclic ion **8**. The reaction requires only 19 kJ/mol. A second mode of formation of ion **8** is provided by the cyclization/hydride shift process **5** → **8**. It turns out that this route is less favorable than the two-step reaction **5** → **6** → **8** by ca. 40 kJ/mol.

Whatever its origin, the radical cation **8** may either lose a hydrogen atom to form the ion **c** or give rise to ionized 1,2-dihydrofulvene, **9**, by simultaneous 1,2-hydrogen shift and ring-opening processes. From Table 5, we can see that the latter channel is favored by 20 kJ/mol. However, a competition between these two reactions may exist because the transition structure of lower energy, **TS 8/9**, corresponds to a rearrangement process, disfavored by an entropy effect, whereas the direct hydrogen loss is characterized by a loose transition stucture, **TS 8/c**. This result is in agreement with the fact that ions **c** are, indeed, detected together with ions **b** during gas-phase titration experiments. Obviously, the latter structure is likely to originate from the radical cation **9**. One should note, however, that, in addition to ions **b**, ions **d** would be competitively produced from the radical cation **9**. However, as indicated in Table 5, formation of **b** is energetically preferred in that **TS 9/b** lies 65 kJ/mol lower in energy than **TS 9/d**.

It is also worth mentioning that ions **a**, **b**, and **c** produced by reaction I with thermalized reactants do not have enough internal energy to interconvert to each other. Indeed, according to our earlier calculations at the G2(MP2) level,[25] isomerization of $C_6H_7^+$ ions **a** into **b** or **c** requires 219 or 171 kJ/mol, respectively. This is significantly higher than the available energy of 133 kJ/mol calculated from the experimental heats of formation of **1**, **2**, **a**, and H$^\bullet$. In fact, only two reactions are allowed to occur from ions **a** with 133 kJ/mol of internal energy, including (i) the 1,2-H shift **a** → **a′**, which requires only 35 kJ/mol, and (ii) the isomerization (by a 1,2-H shift) **b** → **d**, which passes through a transition structure lying 120 kJ/mol higher in energy than **a**.

In considering the potential energy profile sketched in Figure 4, several questions can now be addressed: Why is the reaction efficiency so low (≈10%)? Is the proposed mechanism in accordance with the observed branching ratio of the three product ions?

First, we can see that the formation of the cyclic structure **5** is the energy-determining step common to the all of the hydrogen-atom eliminations. Moreover, **TS 4/5** is a constrained transition structure, which necessarily possesses a slowing effect on the observed reaction rate. This can be illustrated by a simple kinetic model, neglecting the influence of the intermediate **3** on the reaction rate.

$$\mathbf{1} + \mathbf{2} \underset{k_{-1}}{\overset{k_1}{\rightleftharpoons}} \mathbf{4} \underset{k_{-2}}{\overset{k_2}{\rightleftharpoons}} \mathbf{5} \xrightarrow{k_3} C_6H_7^+ + H^\bullet$$

The overall rate constant of this reaction, k_{over}, is given by

$$k_{over} = k_1k_2k_3/(k_{-1}k_3 + k_2k_3 + k_{-1}k_{-2})$$

When considering the critical energies associated with reactions **5** → $C_6H_7^+$ + H$^\bullet$ and **5** → **4**, it is evident that the approximation $k_3 \gg k_{-2}$ applies. Consequently, k_{over} reduces to

$$k_{over} = k_1k_2/(k_{-1} + k_2)$$

and the reaction efficiency is simply given by

$$RE = k_{over}/k_1 = k_2/(k_{-1} + k_2)$$

Because the reaction intermediates **4** and **5** are connected to each other by a tight transition structure, k_2 is smaller than k_{-1}, and the reaction efficiency should be less than unity. This may be quantitatively estimated in the present case.

Unimolecular rate constants k_i can be calculated in the RRKM framework

$$k_i = \sum P^{\ddagger}(E - E_0)/hN(E)$$

where E_0 is the critical energy of the considered step and $\sum P^{\ddagger}(E - E_0)$ and $N(E)$ represent the sum and the density, respectively, of the vibrational states of the transition structure and the reactant. Quantitative estimates of k_i can be made using the vibrational frequencies and the critical energies provided by ab initio calculations. The classical Beyer−Swinehard algorithm[30] was used for the calculation of k_2 using the vibrational frequencies of **TS 4/5**. To evaluate k_{-1}, which is characterized by a loose transition state, we used the statistical phase-space theory developed by Chesnavich et al.[31] and the

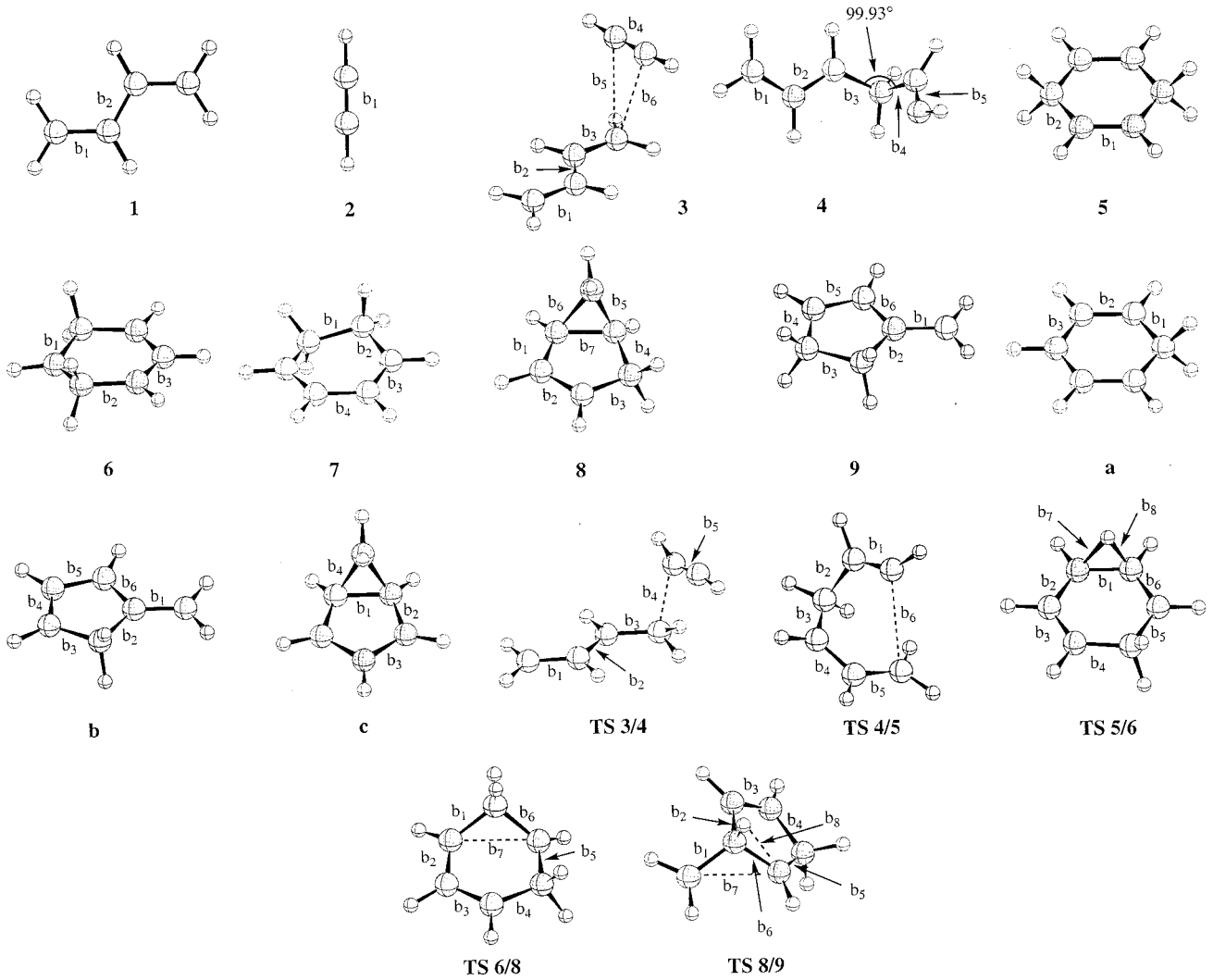

Figure 3. Optimized UMP2/6-31G(d) geometries of the stable and transition structures involved in the mechanistic pathways presented in Scheme 4 (see Table 4 for bond lengths values, b_x).

TABLE 4: UMP2/6-31G(d) Bond Lengths of the Structures Displayed in Figure 3

	bond lengths (in Å)							
structure	b_1	b_2	b_3	b_4	b_5	b_6	b_7	b_8
1	1.382	1.406	–	–	–	–	–	–
2	1.216	–	–	–	–	–	–	–
3	1.371	1.403	1.387	1.221	2.732	2.713	–	–
4[a]	1.357	1.400	1.473	1.531	1.331	–	–	–
5	1.371	1.472	–	–	–	–	–	–
6	1.487	1.471	1.386	–	–	–	–	–
7	1.529	1.475	1.383	1.412	–	–	–	–
8	1.417	1.391	1.486	1.519	1.446	1.632	1.563	–
9	1.398	1.496	1.532	1.475	1.376	1.414	–	–
a	1.464	1.375	1.408	–	–	–	–	–
b	1.360	1.502	1.480	1.383	1.405	1.419	–	–
c	1.474	1.447	1.396	1.561	–	–	–	–
TS 3/4	1.359	1.395	1.423	1.925	1.215	–	–	–
TS 4/5	1.287	1.556	1.455	1.402	1.351	2.774	–	–
TS 5/6	1.415	1.446	1.325	1.493	1.487	1.428	1.380	1.280
TS 6/8	1.485	1.390	1.365	1.475	1.473	1.488	2.293	–
TS 8/9	1.520	1.510	1.317	1.502	1.441	1.449	2.431	2.060

[a] UHF/6-31G(d) optimized geometry.

vibrational and geometrical characteristics of **1** and **2**. In both cases the density of states of the distonic intermediate **4** was used in the rate constant calculation. The two calculated rate constants k_{-1} and k_2 are plotted as a function of the internal energy of the intermediate ion **4** in Figure 5.

It is readily apparent that the forward reaction **4** → **5** (k_2) is considerably disfavored with respect to the reverse reaction leading to **1** + **2** (k_{-1}). Consequently, the reaction efficiency RE is indeed less than unity: its value ranges from 11% for $E = 0.34$ eV to less than 10^{-3}% for $E = 5$ eV. The former situation corresponds to our experimental conditions, i.e., to reactants thermalized at a temperature close to 298 K. As can be seen in Table 1, the agreement with the experimental RE is excellent; it confirms that the tightness of the transition structure **TS 4/5** constitutes the origin of the observed slow rate.

The second point concerns the branching ratio observed among the three product ion structures **a**, **b**, and **c**. The simplified model presented above is, of course, not able to account for the experimental observations as the individual rates of dissociation are not considered. A complete kinetic treatment of the reaction in Scheme 5 would, however, be a considerable task, beyond the scope of the present investigation. Nevertheless, qualitative conclusions can be drawn from the expectation that the rate of formation of each product **a**, **b**, and **c** should be dependent on the rate of dissociation of the relevant intermediate ions **5**−**9**.

The corresponding unimolecular rate constants, k_i, have been calculated using ab initio vibrational frequencies and relative energies of the various species. The results are presented in

TABLE 5: Calculated Total Energies (hartree) and Relative and Zero-Point Energies (kJ/mol) of the Stable and Transition Structures Associated with the Formation of Ions a, b, and c

structure	UMP2/6-311+g(d,p)// UMP2/6-31g(d)	ZPE[b]	S^{2} [c]	ΔE[d]	$\Delta H°_{298}$[e]
1	−155.270312	217	0.911	−	−
2	−77.150513	71	−	−	−
1 + 2	−232.420825	288	−	0	0
3	−232.432231	290	0.896	−28	−38
4	−232.427045[a]	298	1.071[a]	−6[a]	−16[a]
5	−232.530296	308	0.763	−268	−278
6	−233.507792	306	0.765	−224	−234
7	−232.545843	314	0.864	−302	−312
8	−232.528370	310	0.798	−260	−270
9	−232.543279	310	0.872	−300	−310
TS 3/4	−232.419587	289	1.052	+4	−4
TS 4/5	−232.422845	299	1.024	+5	−5
TS 5/6	−232.491924	299	0.877	−175	−185
TS 5/8	−232.476445	301	0.785	−133	−143
TS 6/7	−232.489332[a]	299	0.965[a]	−169[a]	−179[a]
TS 6/8	−232.506016	307	0.839	−205	−215
TS 8/9	−232.458819	293	0.772	−95	−105
TS 5/a	−232.473777	286	0.861	−141	−151
TS 6/a	−232.451052	288	1.078	−79	−89
TS 7/a	−232.467017	289	1.033	−121	−131
TS 8/c	−232.449381	289	0.875	−74	−84
TS 9/b	−232.450520	285	1.158	−81	−91
TS 9/d	−232.423960	280	1.251	−16	−26
a + H$^{\bullet}$	−232.483819	285	−	−169	−173
b + H$^{\bullet}$	−232.469411	283	−	−132	−136
c + H$^{\bullet}$	−232.456026	285	−	−95	−99

[a] Obtained at the UMP2/6-311+G(d,p)//UHF/6-31G(d) level. [b] Zero-point energies based on UHF/6-31G(d) harmonic vibrational wavenumbers and scaled by 0.91. [c] Values obtained at the UMP2/6-311+G(d,p)//UMP2/6-31G(d) level. [d] Relative energies including UMP2/6-311+G(d,p) values and ZPE corrections. [e] Deduced from $\Delta E°_{298}$ by taking into account translational and rotational enthalpic corrections calculated at the UHF/6-31G(d) level.

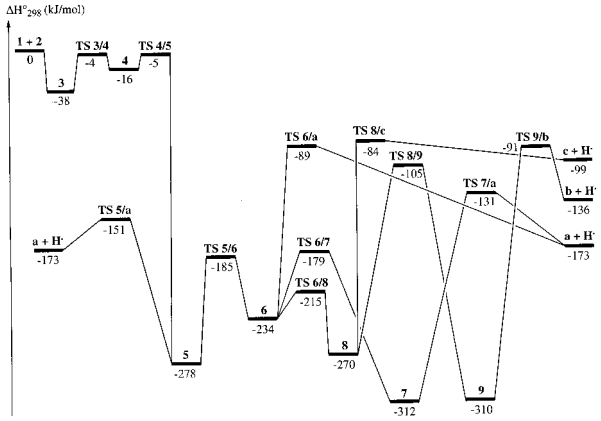

Figure 4. Enthalpy diagram associated with the mechanistic pathways presented in Scheme 4.

Figure 6 on a common energy scale related to the ground state of structure **5**. On this energy scale, the energy level of the reactants **1** + **2** is equal to 2.88 eV.

Examination of Figure 6 reveals that formation of structure **a** (k_5, k_6, and k_7) is consistently favored over that of ions **b** (k_9) or **c** (k_8). Furthermore, the latter two products are produced at comparable rates. These two points are in keeping with the experimental observations that structure **a** is the major product and that **b** and **c** are produced in comparable yields from the reaction between ionized butadiene and neutral acetylene.

The behavior of ionized cyclohexadienes can also be explained from the potential energy profile presented in Figure 4

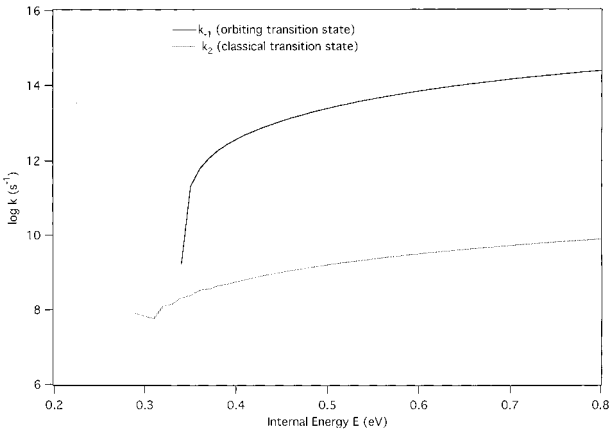

Figure 5. Rate constants of dissociation, k_{-1}, and isomerization, k_2, of structure **4** (see text).

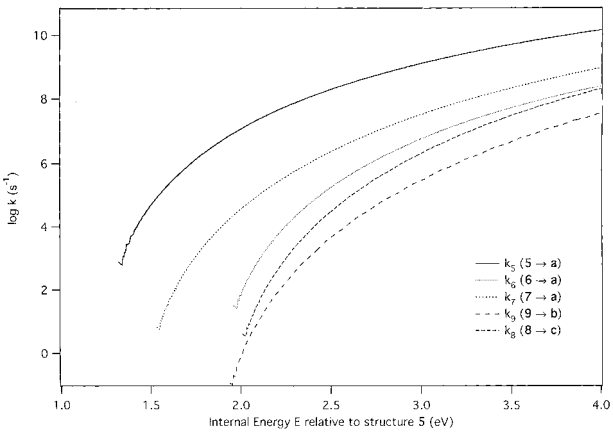

Figure 6. Comparison of the rate constants of dissociation of structures **5**−**9** (see text).

and the rate constants presented in Figure 6. First, a facile interconversion is expected between **5** and **7** via the distonic ion **6**, with isomerization barriers well below the dissociation limits. Second, from both **5** and **7**, formation of structure **a** is favored (k_5 and k_7, respectively; Figure 6), particularly at low energies. At high internal energy, the competitive formation of ions **b** and **c** is predicted. These conclusions are in good agreement with the earlier experiments reported by Lias and Ausloos.[14]

Conclusion

We have shown that the product of the ion−molecule reaction between the butadiene radical cation and acetylene is a mixture of $[C_6H_7]^+$ ions. A gas-phase ion titration procedure was applied in order to (i) identify each isomer by means of its deprotonation energy and (ii) estimate the relative amount of each component. Complete structural assignment was made possible by a comparison with data provided by ab initio molecular orbital calculations. It is unambiguously demonstrated that the major product is the benzenium ion **a**, the most stable of the protonated forms of benzene. The two other identified isomers, **b** and **c**, are the two most stable protonated forms of fulvene.

The calculated potential energy surface [at the UMP2/6-311+G(d,p)//UMP2/6-31G(d) level] is in good accord with the experimental observations. The low efficiency of the reaction and the qualitative product yields are well reproduced by statistical rate calculations using the ab initio calculated parameters. From a mechanistic point of view, it is shown that this Diels−Alder type reaction follows a stepwise process

involving successive bond formations to generate ionized 1,4-cyclohexadiene, which, in turn, may dissociate to give benzenium ion **a**. Hydrogen-atom migrations and a ring-contraction process lead to the $C_6H_8^{+\bullet}$ isomers at the origin of pathways generating the two other product ions, **b** and **c**.

Acknowledgment. The authors are indebted to the Ecole Polytechnique and the FWO-Vlaanderen for financial support.

References and Notes

(1) Fleming, I. *Frontier Orbitals and Organic Chemical Reactions*; Wiley: New York, 1977.

(2) For recent reviews, see: (a) Müller, F.; Mattay, J. *Chem. Rev.* **1993**, *93*, 99. (b) Bauld, N. L. *Tetrahedron* **1989**, *45*, 5307. (c) Fox, M. A., Chanon, M., Eds. *Photoinduced Electron-Transfer Reactions*; Elsevier: Amsterdam, 1988.

(3) For recent studies, see: (a) Hintz, S.; Heidbreder, A.; Mattay, J. *Top. Curr. Chem.* **1996**, *177*, 77. (b) Peglow, T.; Blechert, S.; Steckhan, E. *Chem. Eur. J.* **1998**, *4*, 107. (c) Gürtler, C. F.; Blechert, S.; Steckhan, E. *Angew. Chem., Intl. Ed. Engl.* **1995**, *34*, 1900. (d) Schmittel, M.; Wöhrle, C.; Bohn, I. *Chem. Eur. J.* **1996**, *2*, 1031.

(4) Bauld, N. L. *J. Am. Chem. Soc.* **1992**, *114*, 5800.

(5) (a) Hoffmann, M.; Schaefer, H. F., III *J. Am. Chem. Soc.* **1999**, *121*, 6719. (b) Haberl, U.; Wiest, O.; Steckhan, E. *J. Am. Chem. Soc.* **1999**, *121*, 6730.

(6) For recent studies on gas-phase pericyclic reactions of radical cations, see: (a) Dass, C. *Mass Spectrom. Rev.* **1990**, *9*, 1. (b) Smith, R. L.; Chou, P. K.; Kenttämaa, H. I. In *The Structure, Energetics and Dynamics of Organic Ions*; Baer, T., Ng, C. Y., Powis, I., Eds.; John Wiley: New York, 1996. (c) Eberlin, M. N.; Sorrilha, A. E. P. M.; Gozzo, F. C.; Pimpim, R. S. *J. Am. Chem. Soc.* **1997**, *119*, 3550. (d) Nixdorf, A.; Grützmacher, H. F. *J. Am. Chem. Soc.* **1997**, *119*, 6544. (e) de Visser, S. P.; de Koning, L. J.; Nibbering, N. M. M. *J. Am. Chem. Soc.* **1998**, *120*, 1517. (f) Jungwirth, P.; Bally, T. *J. Am. Chem. Soc.* **1993**, *115*, 5783. (g) Hrouda, V.; Carsky, P.; Ingr, M.; Chval, Z.; Sastry, G. N.; Bally, T. *J. Phys. Chem.* **1998**, *102*, 9297.

(7) (a) Bouchoux, G.; Penaud-Berruyer, F. *Org. Mass Spectrom.* **1993**, *28*, 421. (b) Bouchoux, G.; Penaud-Berruyer, F. *Org. Mass Spectrom.* **1994**, *29*, 366. (c) Bouchoux, G.; Salpin, J. Y. *Rapid Commun. Mass Spectrom.* **1994**, *8*, 325. (d) Bouchoux, G.; Salpin, J. Y. *Rapid Commun. Mass Spectrom.* **1997**, *11*, 1001.

(8) (a) Hofmann, M.; Schaefer, H. F., III *J. Phys. Chem.* Submitted for publication. (b) Bouchoux, G.; Salpin, J. Y.; Baer, T.; Li, Y. Unpublished work.

(9) (a) Bakhtiar, R.; Drader, J. D.; Jacobson, D. B *J. Am. Chem. Soc.* **1992**, *114*, 8304. (b) Schroeter, C. A.; Schalley, R.; Wesendrup, R.; Schröder, D.; Schwarz, H. *Organometallics* **1997**, *16*, 986.

(10) Alleman, M.; Kellerhals, H. P.; Wanczek, K. P.; Koffel, P. *Int. J. Mass Spectrom. Ion Processes* **1985**, *65*, 97.

(11) Bartmess, J. E.; Georgiadis, R. M. *Vacuum* **1983**, *33*, 149.

(12) Frisch, M. J.; Trucks, G. W.; Schlegel, H. B.; Gill, P. M. W.; Johnson, B. G.; Robb, M. A.; Cheeseman, J. R.; Keith, T.; Petersson, G. A.; Montgomery, J. A.; Raghavachari, K.; Al-Laham, M. A.; Zakrzewski, V. G.; Ortiz, J. V.; Foresman, J. B.; Cioslowski, J.; Stefanov, B. B.; Nanayakkara, A.; Challacombe, M.; Peng, C. Y.; Ayala, P. Y.; Chen, W.; Wong, M. W.; Andres, J. L.; Replogle, E. S.; Gomperts, R.; Martin, R. L.; Fox, D. J.; Binkley, J. S.; Defrees, D. J.; Baker, J.; Stewart, J. P.; Head-Gordon, M.; Gonzalez, C.; Pople, J. A. *Gaussian 94*, revision E.2; Gaussian, Inc.: Pittsburgh, PA, 1995.

(13) Scott, A. P.; Radom, L. *J. Phys. Chem.* **1996**, *100*, 16502.

(14) Curtiss, L. A.; Raghavachari, K.; Pople, J. A. *J. Chem. Phys.* **1993**, *98*, 1293.

(15) Smith, B. J.; Radom, L. *Chem. Phys. Lett.* **1994**, *231*, 345.

(16) Miller, K. J. *J. Am. Chem. Soc.* **1990**, *112*, 8533.

(17) Su, T.; Bowers, M. T. In *Gas-Phase Ion Chemistry*; Academic Press: New York, 1979; Vol. 1, p 83.

(18) Herman, J. A.; Herman, R.; McMahon, T. B. *Can. J. Chem.* **1991**, *69*, 2038.

(19) Lias, S. G.; Ausloos, P. *J. Chem. Phys.* **1985**, *82*, 3613.

(20) Lias, S. G.; Hunter, E. P. L. *J. Phys. Chem. Ref. Data* **1998**, *27*, 413.

(21) Kuck, D.; Schneider, J.; Grützmacher, H. F. *J. Chem. Soc., Perkin Trans. 2* **1985**, 689.

(22) Depuy, C. H.; Gareyec, R.; Fornarini, S. *Int. J. Mass Spectrom. Ion Processes* **1997**, *161*, 41.

(23) Lias, S. G.; Bartmess, J. E.; Liebman, J. F.; Holmes, J. H.; Levin, R. D.; Mallard, W. G. *J. Phys. Chem. Ref. Data* **1988**, *17*, Supplement 1.

(24) Szulejko, J. E.; McMahon, T. B. *J. Am. Chem. Soc.* **1993**, *115*, 7839.

(25) Bouchoux, G.; Yanez, M.; Mo, O. *Int. J. Mass Spectrom.* **1998**, *185/186/187*, 241.

(26) Büker, H. H.; Grützmacher, H. F.; Crestoni, M. E.; Ricci, A. *Int. J. Mass Spectrom. Ion Processes* **1997**, *160*, 167.

(27) Bouchoux, G.; Salpin, J.-Y.; Leblanc, D. *Int. J. Mass Spectrom. Ion Processes* **1996**, *153*, 37.

(28) A curve-fitting procedure involving a nonlinear iterative least-squares method (IGOR Pro, Wavemetrics Inc.) was used. An *RT* value of 5.0 kJ/mol (ref 22) was assumed during the fitting, all the other parameters being free of constraint.

(29) (a) Wong, M. W.; Pross, A.; Radom, L. *J. Am. Chem. Soc.* **1994**, *116*, 6284. (b) Zytowsky, T.; Fischer, H. *J. Am. Chem. Soc.* **1996**, *118*, 437.

(30) (a) Beyer, T.; Swinehard, D. R. *ACM Commun.* **1973**, *16*, 379. (b) Stein, S. E.; Rabinovitch, B. S. *J. Chem. Phys.* **1973**, *58*, 2438.

(31) Chesnavich, W. J.; Bass, L.; Grice, M. E.; Song, K.; Webb, D. A. *TSTPST: Statistical Theory Package for RRKM/QET/TST/PST Calculations*; QCPE program 557 (http://qcpe.chem.indiana.edu/).